Proc. Natl. Acad. Sci. USA
Vol. 95, pp. 7993–7998, July 1998
Biochemistry

Gp91^{phox} is the heme binding subunit of the superoxide-generating NADPH oxidase

LIXIN YU*, MARK T. QUINN†, ANDREW R. CROSS‡, AND MARY C. DINAUER*§

*Wells Center for Pediatric Research, Indiana University School of Medicine, Indianapolis, IN 46202; †Department of Veterinary Molecular Biology, Montana State University, Bozeman, MT 59717; and ‡Department of Molecular and Experiment Medicine, The Scripps Research Institute, La Jolla, CA 92037

Edited by Seymour J. Klebanoff, University of Washington School of Medicine, Seattle, WA, and approved May 12, 1998 (received for review April 2, 1998)

ABSTRACT **The phagocyte NADPH oxidase flavocytochrome b_{558} is a membrane-bound heterodimer comprised of a glycosylated subunit, gp91^{phox}, and a nonglycosylated subunit, p22^{phox}. It contains two nonidentical heme groups that mediate the final steps of electron transfer to molecular oxygen (O_2), resulting in the generation of superoxide ion (O_2^-). However, the location of the hemes within the flavocytochrome heterodimer remains controversial. In this study, we have used transgenic COS7 cell lines expressing gp91^{phox}, p22^{phox}, or both polypeptides to examine the relative role of each flavocytochrome b_{558} subunit in heme binding and O_2^- formation. A similar membrane localization was observed when gp91^{phox} and p22^{phox} were either expressed individually or coexpressed, as analyzed by confocal microscopy and immunoblotting of subcellular fractions. Spectral analysis of membranes prepared from COS7 cell lines expressing either gp91^{phox} or both gp91^{phox} and p22^{phox} showed a *b*-type cytochrome with spectral characteristics identical to those of human neutrophil flavocytochrome b_{558}. In contrast, no heme spectrum was detected in wild-type COS7 membranes or those containing only p22^{phox}. Furthermore, redox titration studies suggested that two heme groups were contained in gp91^{phox} expressed in COS7 membranes, with midpoint potentials of −264 and −233 mV that were very similar to those obtained for neutrophil flavocytochrome b_{558}. These results provide strong support for the hypothesis that gp91^{phox} is the sole heme binding subunit of flavocytochrome b_{558}. However, coexpression of gp91^{phox} and p22^{phox} in COS7 membranes was required to support O_2^- production in combination with neutrophil cytosol, indicating that the functional assembly of the active NADPH oxidase complex requires both subunits of flavocytochrome b_{558}.**

The phagocyte NADPH oxidase plays a crucial role in host defense against invading microorganisms by catalyzing the formation of superoxide (O_2^-), which is the precursor of a variety of microbicidal oxidants such as hydrogen peroxide (H_2O_2) (1). This enzyme complex consists of a membrane-bound flavocytochrome b_{558} and three cytosolic proteins (p47^{phox}, p67^{phox}, and a small GTP-binding protein Rac1/Rac2), which are translocated to the plasma membrane during assembly of the active enzyme complex (2). Large quantities of O_2^- then are generated by the transfer of electrons from cytosolic NADPH to molecular O_2 (3). The physiological significance of the phagocyte NADPH oxidase in host defense is illustrated by the severe recurrent bacterial and fungal infections that occur in patients with chronic granulomatous disease whose phagocytes are unable to generate O_2^- because of various mutations in four of the oxidase proteins (gp91^{phox}, p22^{phox}, p47^{phox}, and p67^{phox}) (1).

The redox center of the oxidase is a unique low potential *b*-type flavocytochrome, flavocytochrome b_{558} (also known as flavocytochrome b_{-245}), which is found almost exclusively in phagocytic cells. Flavocytochrome b_{558} is comprised of two integral membrane proteins, a glycosylated 91-kDa glycoprotein (gp91^{phox}), encoded by the gene affected in the X-linked form of chronic granulomatous disease, and a nonglycosylated 22-kDa subunit (p22^{phox}), which is affected in an autosomal recessive form of the disease (1). Both physical studies and peptide sequencing of purified flavocytochrome b_{558} indicate that it is a heterodimer with stoichiometry of 1:1 (4–6). Flavocytochrome b_{558} contains both flavin and heme groups that participate in the sequential transfer of electrons from NADPH to O_2, although p67^{phox} also may contain an NADPH binding site (7). The hydrophilic carboxyl-terminal half of gp91^{phox} contains motifs with homology to the flavin- and NADPH-binding domains of ferredoxin NADP$^+$ reductase (8–10). There also appear to be two nonidentical heme groups per flavocytochrome b_{558} heterodimer, with midpoint redox potentials (Em) of −225 and −265 mV (11). These hemes are embedded within the membrane (12) and are coordinated noncovalently by histidines in both heme axial positions (13–15).

It remains uncertain as to which of the two flavocytochrome subunits bears the heme prosthetic groups. The gp91^{phox} and p22^{phox} polypeptides in purified flavocytochrome b_{558} are closely associated and are separable only under denaturing conditions that typically result in the loss of heme binding (4). Heterodimer formation appears to be important for stable expression of each subunit in neutrophils because virtually all patients with flavocytochrome b_{558} mutations lack both gp91^{phox} and p22^{phox} polypeptides, regardless of which subunit is affected by the genetic defect (16). Inhibition of heme biosynthesis also results in a marked decrease in flavocytochrome b_{558} expression, suggesting that heme incorporation influences heterodimer formation (17). Several reports have suggested that p22^{phox} is the heme-binding subunit (18–19), although there is only a single invariant histidine in p22^{phox} (20). Quinn *et al.* (12) demonstrated heme staining in both gp91^{phox} and p22^{phox} by using low temperature lithium dodecyl sulfate/PAGE to fractionate purified flavocytochrome b_{558} and proposed that one heme resides within gp91^{phox} and that the second may be shared between both gp91^{phox} and p22^{phox} (12).

We recently developed an approach to examine the relative function of each flavocytochrome b_{558} subunit by using the transgenic expression of gp91^{phox} and p22^{phox} in monkey kidney COS7 cells or murine 3T3 fibroblasts, which lack endogenous p22^{phox} and gp91^{phox} expression (17). The unassembled polypeptides appear to be more stable in nonphagocytic cells, perhaps because of differences in the proteolytic environment, although coexpression of p22^{phox} and gp91^{phox} increases the abundance of the mature 91-kDa form of gp91^{phox} (17). In the studies presented here, we have used transgenic COS7 cell lines that express gp91^{phox}, p22^{phox}, or both polypeptides to investigate the relative participation of gp91^{phox} and p22^{phox} in heme binding and in O_2^-

The publication costs of this article were defrayed in part by page charge payment. This article must therefore be hereby marked "*advertisement*" in accordance with 18 U.S.C. §1734 solely to indicate this fact.

This paper was submitted directly (Track II) to the *Proceedings* office.
Abbreviations: *phox*, *ph*agocyte *ox*idase; Em, midpoint redox potential.
§To whom reprint requests should be addressed at: Wells Center, Room 466, Cancer Research Institute, 1044 W. Walnut Street, Indianapolis, IN 46202. e-mail: mdinauer@iupui.edu.

formation. We found that gp91^{phox} expressed in the absence of p22^{phox} was targeted correctly to the plasma membrane and exhibited a reduced minus oxidized difference heme spectrum that was identical to that of neutrophil flavocytochrome b_{558}. Furthermore, redox titration analysis suggested that gp91^{phox} alone contained two heme groups with midpoint potentials of −233 and −264 mV, almost identical to those seen for the neutrophil flavocytochrome b_{558}. However, coexpression of gp91^{phox} and p22^{phox} were required to support O_2^- generation in the cell-free NADPH oxidase assay, indicating that the functional assembly of the active enzyme complex still requires both subunits of flavocytochrome b_{558}.

MATERIALS AND METHODS

Materials. Anthraquinone 2,6-disulfonate, duroquinone, 2-hydroxy-1,4-napthoquinone, and 2,3,5,6-tetramethylphenylenediamine were obtained from Aldrich. Anthraquinone and octyl-β-D-glucopyranoside were supplied by Fluka and Calbiochem, respectively. Pyocyanine was synthesized as described (11). Fluorescein isothiocyanate-conjugated goat anti-mouse IgG were purchased from Boehringer Mannheim. All other reagents were from Sigma.

Transgenic Expression of gp91^{phox} and p22^{phox} in COS7 Cells. COS7 cell lines expressing gp91^{phox}, p22^{phox}, or both flavocytochrome b_{558} subunits were made previously by stable transfection of the corresponding full length cDNAs into parental COS7 wild-type cells (COS7 WT) that lack endogenous expression of gp91^{phox} and p22^{phox} (17). These derivative COS7 lines are referred to as COS7 p22, COS7 gp91, and COS7 gp91/p22. The expression of recombinant gp91^{phox} and p22^{phox} in these transfectants was examined by immunoblotting as described (17). Cellular membrane and cytosolic fractions were prepared by sequential centrifugation after cell disruption by sonication (21). Confocal microscopy also was used to determine the subcellular localization of gp91^{phox} and p22^{phox}. Mouse mAb 7D5, (22, 23) (kindly provided by M. Nakamura, Nagasaki Univ.), which recognizes an extracellular epitope (A. Yamauchi, L.Y., A. Potgen, F. Kuribayashi, S. Kanegasaki, D. Roos, M.D., and M. Nakamura, unpublished work) of gp91^{phox}, and mouse mAb 449, which reacts with a intracellular domain of p22^{phox} (24, 25) (kindly provided by D. Roos and A. Verhoeven, Central Laboratory of The Netherlands Blood Transfusion Service), were used as primary antibodies in the staining of unpermeabilized and permeabilized cells. For membrane permeabilization, cells were treated with 0.01% saponin for 10 min after blocking and maintained with the same concentration of saponin in the subsequent incubation with the primary antibody before fixation with 1% of paraformaldehyde and staining with the secondary antibody. After the incubation with fluorescein isothiocyanate-conjugated secondary antibody, cells were observed by confocal microscopy (26). Mouse IgG1 was used in parallel as an isotype control.

Spectral Analysis of Flavocytochrome b_{558} Expressed in COS7 Cells. Membranes prepared from WT and transfected COS7 cells were extracted with 2% octyl glucoside as described for human neutrophil flavocytochrome b_{558} (4). In brief, COS7 cell membranes were treated with 1 M NaCl and centrifuged at 100K × *g* for 40 min at 4°C. The resulting pellet then was sonicated into Relax buffer (10 mM Hepes, pH 7.4/100 mM KCl/10 mM NaCl) containing 1 mM EDTA, 1 mM phenylmethylsulfonyl fluoride, 10 μg/ml chymostatin, and 2% octyl glucoside. The membranes were extracted for 30 min on ice, and the mixture was centrifuged at 100K × *g* for 40 min at 4°C. The 2% octyl glucoside supernatant then was diluted 1:1 in Relax buffer and analyzed by dithionite-reduced minus oxidized difference spectroscopy on a Cary 3E dual-beam spectrophotometer (Varian) by using an extinction coefficient of 21.6 mM^{-1} cm^{-1} (27). Samples were reduced by mixing several grains of sodium dithionite into the cuvette.

Measurement of Oxidation–Reduction Potentials. Potentiometric titrations were performed in a stirred cuvette fitted with platinum and calomel electrodes under an atmosphere of oxygen-free argon by using the apparatus described previously (11, 28) in a final volume of 1.6 ml. Samples were prepared by solubilizing salt-washed membranes from 4.0×10^8 cells in 100 mM KCl, 50 mM Mops buffer (pH 7.0) containing 1.0% wt/vol octyl glucoside. Detergent-insoluble material was removed by centrifugation at 100k × *g* for 40 min. Absorbance spectra were recorded between 580 and 530 nm, by using a Perkin–Elmer Lambda 18 spectrophotometer, at a series of electrode potentials (11). The potential was adjusted with small ≪ microliter volumes of solutions of sodium dithionite (reductive titrations) or potassium ferricyanide (oxidative titrations). The degree of reduction of flavocytochrome b_{558} was estimated by the height of the absorbance band at 558 nm relative to a baseline drawn between 530 and 570 nm. These absorbances were plotted against electrode potential. The best fit to the data points was calculated by using the GRAPHPAD Prism software package (San Diego, CA).

Analysis of NADPH Oxidase Activity in a Cell-Free Assay. NADPH oxidase activity was measured in a cell-free assay system by using both cytochrome *c* and chemiluminescence detection systems. To analyze O_2^- generation in a cytochrome *c*-based system, partially purified, reflavinated, and relipidated flavocytochrome b_{558} from COS7 gp91/p22 was incubated with human neutrophil cytosol, and O_2^- formation was monitored by the superoxide dismutase-inhibitable reduction of cytochrome *c* as described (29). To test whether COS7 membranes interfered with O_2^- production or detection, we also added COS7 membranes to a system consisting of 0.5 mM xanthine and 0.01 units/ml xanthine oxidase. Addition of either COS7 WT or COS7 gp91/p22 membranes (50 μg/ml) to this system had little effect on superoxide dismutase-inhibitable O_2^- production (not shown).

For enhanced sensitivity, we also analyzed O_2^- generation by using a chemiluminescence detection system. In these assays, we added 30 mM lucigenin, 450 μg/ml COS7 cell membranes (≈1×10^6 cell equivalents/ml), and 8×10^6 cell equivalents/ml human neutrophil cytosol to a standard cell-free assay system (21), incubated for 2 min, and then added 150 μM SDS. After 3 min, 200 μM NADPH was added, and the rate of O_2^- production was measured continuously by monitoring chemiluminescence by using a Lumat LB 9507 luminometer (Wallac, Gaithersburg, MD). The data, collected as relative luminescence units, were plotted versus time, and the area under the curve was used for analysis (30). As a positive control, we analyzed 40 μg/ml human neutrophil membranes (≈2×10^7 cell equivalents/ml) instead of COS7 cell membranes. Specificity was demonstrated by the addition of 10 mM Tiron, an O_2^- scavenger, which served as the negative control. In reaction mixtures containing everything except cytosol, relative luminescence units remained at background levels throughout the assay period (15 min).

RESULTS

Expression of gp91^{phox} and p22^{phox} in Transfected COS7 Cells. By using transgenic techniques, we have generated COS7 cell lines with stable expression of the individual flavocytochrome b_{558} subunits gp91^{phox} (COS7 gp91) and p22^{phox} (COS7 p22), as well as a line expressing both subunits (COS7 gp91/p22) (17). To determine the subcellular location of each flavocytochrome subunit, we stained COS7 WT and transfected derivative cells with a mAb, 7D5, that reacts with an extracellular epitope of gp91^{phox}, and a mAb, 449, that reacts with a intracellular epitope of p22^{phox} and examined the cells by confocal microscopy. As seen in Fig. 1*A*, the 7D5 antibody stained the cell surface of COS7 gp91 and COS7 gp91/p22 cells but not COS7 p22 and COS7 WT cells. The p22^{phox} antibody 449 produced a reticular staining pattern that was diffuse but was excluded from the nucleus in saponin-permeabilized COS7 p22 and COS7 gp91/p22 cells. A similar distribution of gp91^{phox} was seen in saponin-permeabilized COS7 gp91 and COS7 gp91/p22 cells stained with the gp91^{phox}-specific 7D5 antibody (not shown). Immunoblot analysis of cytosol and

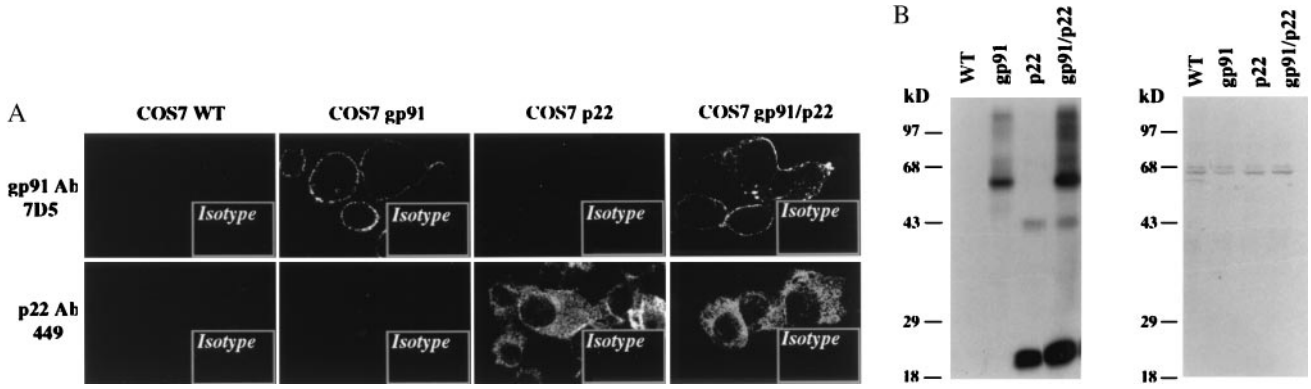

FIG. 1. Localization of gp91^{phox} and p22^{phox} in WT and transgenic COS7 cells. (*A*) Cells were labeled with mAb 7D5, which recognizes an extracellular epitope of gp91^{phox}, or mAb 449, which recognizes an intracellular epitope on p22^{phox}. For staining with mAb 449, the cells were permeabilized with saponin as described under *Materials and Methods*. After incubation with a fluorescein isothiocyanate-conjugated secondary antibody, cells were observed by confocal microscopy. Mouse IgG1 was used in parallel as an isotype control in the cell staining. (Imaging amplifications: ×360 for 7D5 and 449 antibody staining and ×148 for IgG1 staining.) (*B*) Cellular membrane (*Left*) and cytosolic fractions (*Right*) prepared from the indicated COS7 cells were analyzed for gp91^{phox} and p22^{phox} expression by immunoblotting with a mixture of mAbs for gp91^{phox} (24) and p22^{phox} (24). Each lane was loaded with 10 μg of protein. The band ≈44 kDa in the COS7 p22 and COS7 gp91/p22 lanes represents dimeric aggregate of p22^{phox}.

cellular membranes prepared from parental and transfected COS7 cells demonstrated that expression of p22^{phox} and gp91^{phox} was localized exclusively to the membrane fraction (Fig. 1*B*). Hence, the reticular staining pattern seen for gp91^{phox} and p22^{phox} in permeabilized COS7 cells likely represents intracellular membranes. No positive signals were observed with the mAb 449 in unpermeabilized COS7 p22, COS7 gp91/p22, COS7 WT, or COS7 gp91 cells (not shown).

The levels of gp91^{phox} and p22^{phox} expression in COS7 cells also were determined by densitometric analysis. The flavocytochrome heterodimer was expressed at ≈30% compared with normal neutrophils (not shown). Gp91^{phox} alone, in the absence of its partner p22^{phox}, was expressed at a lower level, ≈30–50% of that seen in COS7 cells coexpressing gp91^{phox} and p22^{phox}.

Gp91^{phox} Contains Both Heme Moieties of Flavocytochrome b$_{558}$. To further characterize the flavocytochrome expressed in COS7 cells, we analyzed detergent extracts of COS7 cell membranes by using reduced minus oxidized difference spectroscopy. We also included samples of partially purified human neutrophil flavocytochrome b_{558} in our analysis for comparison. As shown in Fig. 2*A*, the COS7 gp91/p22 (red line) and COS7 gp91 (green line) cell membranes contained a *b*-type cytochrome with spectral characteristics similar to those of human neutrophil flavocytochrome b_{558} (blue line). The spectra of COS7 p22 (black line) and COS7 WT (not shown) were identical and showed no evidence of a heme spectrum. Comparison of the heme spectra from COS7 gp91/p22 and COS7 gp91 with that of authentic human neutrophil flavocytochrome b_{558} confirmed that all three spectra were essentially identical with respect to the locations of the α (558.5–559 nm), β (529–530 nm), and Soret (426.5–427 nm) band absorbance peaks (see Fig. 2 *B* and *C* for enlarged views of the Soret and α band peaks). The specific activities of the flavocytochrome were 1.79 and 0.950 nmol/mg protein in COS7 gp91/p22 and COS7 gp91 membrane extracts, respectively. As with neutrophil membranes, if we omitted the 1 M NaCl wash before octyl glucoside extraction, we obtained lower specific activities (0.950 and 0.726 nmol/mg protein for COS7 gp91/p22 and COS7 gp91, respectively). In any case, the specific activities determined for COS7 gp91/p22 were very similar to those previously determined by Parkos and coworkers (4) for human neutrophil membrane extracts.

We have shown previously that the neutrophil flavocytochrome b_{558} contains two nonidentical hemes with Em of −225 and −265 mV (11). Having established that gp91^{phox} is capable of binding heme in the absence of p22^{phox} (Fig. 2), it was clearly of interest to determine which heme(s) were present in gp91^{phox} and whether the midpoint potential(s) were the same as in the native gp91^{phox}/p22^{phox} heterodimer. As shown in Fig. 3, redox titrations of COS7 gp91/p22 samples could be fitted most accurately to redox components with Em of −235 and −260 mV. These values were very close to the values previously determined for flavocytochrome b558 purified from human neutrophil membranes (−225 and −265 mV) (11). Surprisingly, redox titrations of COS7 gp91phox samples were indistinguishable from those of COS7 gp91/p22 (Fig. 3) and also could be fitted to two components with Em of −233 and −264 mV ($R^2 = 0.992$). A single component fit gave an Em of −249 mV ($R^2 = 0.988$, not shown). No absorbance changes attributable to flavocytochrome could be detected in samples from COS7 WT or COS7 p22 membranes (not shown). Thus, it appears that both heme groups are contained within gp91^{phox} alone, neither being shared with p22^{phox} as was hypothesized previously.

Functional Analysis of gp91^{phox} and p22^{phox} in COS7 Cell Lines. We next examined the ability of gp91^{phox} and p22^{phox}, either

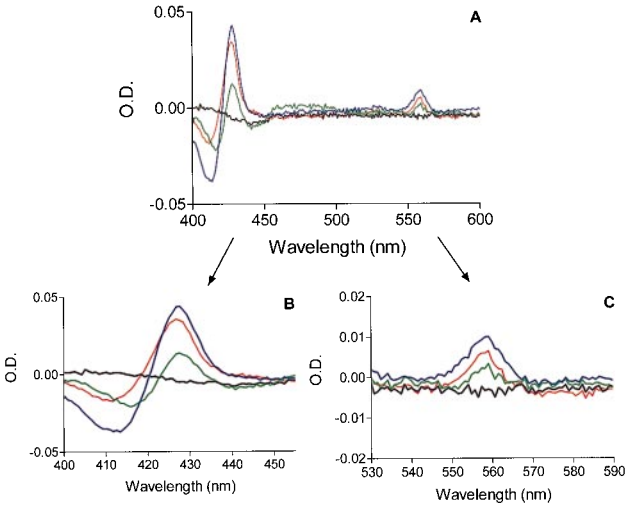

FIG. 2. Dithionite-reduced minus oxidized difference spectra of COS7-expressed flavocytochrome b_{558}. (*A*) solubilized samples of COS7 p22 (black line), COS7 gp91 (green line), COS7 gp91/p22 (red line), and human neutrophil flavocytochrome b_{558} (blue line) were analyzed by difference spectroscopy as described under *Materials and Methods*. Samples of COS7 WT (not shown) had identical spectra to those shown for COS7 p22. (*B* and *C*) show enlarged views of the Soret- and α-band regions, respectively. Representative of triplicate analyses from three separate membrane preparations.

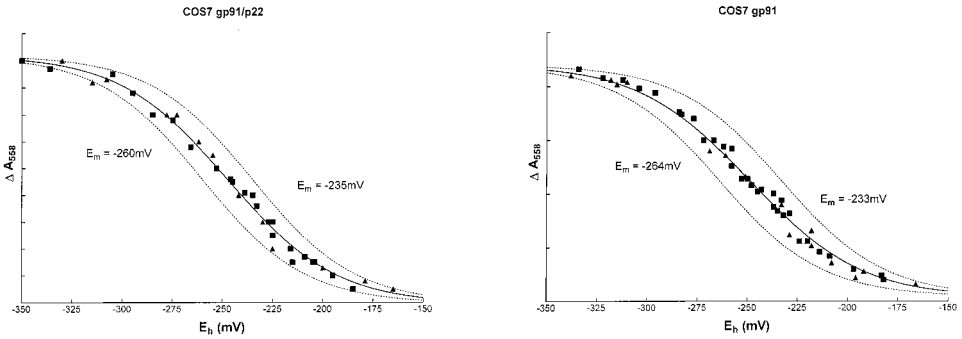

FIG. 3. Potentiometric titrations of solubilized COS7 gp91/p22 and COS7 gp91 membranes. Oxidation–reduction potential measurements were performed on COS7 gp91/p22 (*Left*) and COS7 gp91 (*Right*) membranes as described under *Materials and Methods*. Potassium ferricyanide was used for oxidative titrations (square), and sodium ditionite was used for reductive titrations (triangle). The solid curves are the best fits to the data points for two components; the dashed curves represent the contributions of the individual heme centers, each contributing ≈50% to the absorbance change. Data from the redox titrations was fitted by nonlinear regression (Marquardt method) to the Nernst equation by using GRAPHPAD Prism software. Initial estimated values for the variables were the maximum absorbance change of each component and its corresponding midpoint potential. The total absorbance change in both cases was ≈0.01 absorbance units.

when expressed as individual polypeptides or when coexpressed in COS7 cells, to support O_2^- production. To address this question, we used a cell-free NADPH oxidase assay system by using human neutrophil cytosol and COS7 cell membranes. As shown in Table 1, only membranes prepared from COS7 gp91/p22 were able to reconstitute NADPH oxidase activity as measured by using a chemiluminesence assay for O_2^- formation, and COS7 gp91 and COS7 p22 membranes exhibited no activity above the background shown by COS7 WT membranes. The absolute level of oxidase activity produced by COS7 gp91/p22 cell membranes was ≈50% of that produced by neutrophil membranes. However, on a membrane protein basis, the COS7 gp91/p22 oxidase activity was only ≈10% of that generated by human neutrophil membranes. To confirm our chemiluminescence results and obtain quantitative measurements of the amount of O_2^- produced, we also used a cytochrome *c*-based assay. Cell-free assays using neutrophil cytosol combined with partially purified gp91*phox*, p22*phox*, or gp91*phox*/p22*phox* isolated from the corresponding COS7 cell membranes showed similar results (Table 1), although a slightly higher level of O_2^- (≈20%) was generated by using partially purified gp91*phox*/p22*phox* in this type of assay. Although equivalent fractions from COS7 gp91 contained spectrally detectable heme that was similar in amount to that from COS7 gp91/p22, no O_2^- could be detected. Thus, at least a portion of the gp91*phox*/p22*phox* heterodimer expressed in COS7 gp91/p22 cell membranes is functionally capable of supporting a respiratory burst in the presence of human neutrophil cytosol. In addition, these results indicate that, even though COS7 gp91 exhibits a characteristic flavocytochrome b_{558} heme spectrum, both gp91*phox* and p22*phox* are required for the active NADPH oxidase.

DISCUSSION

The NADPH oxidase flavocytochrome b_{558} mediates the terminal steps in electron transfer, resulting in the generation of O_2^- during the phagocyte respiratory burst. The relative functions of its two integral membrane protein subunits, gp91*phox* and p22*phox*, have been characterized incompletely because stable expression of each subunit in phagocytes depends on heterodimer formation. However, gp91*phox* and p22*phox*, expressed from stable transgenes, appear to be more stable as unassembled polypeptides in heterologous cell lines compared with phagocytic cells (17). In the current study, we have used transgenic COS7 cell lines to examine the subcellular localization, heme binding, and functional capacity of each flavocytochrome b_{558} subunit when expressed in the absence of its partner.

The gp91*phox* subunit of flavocytochrome b_{558} is a glycoprotein that undergoes glycosylation in the endoplasmic reticulum, with subsequent modification and processing of carbohydrate within the Golgi as it is transported to the plasma membrane (17, 31). We had shown previously that maturation of high mannose carbohydrates to complex oligosaccharides on gp91*phox* can occur in the absence of p22*phox* when recombinant gp91*phox* is expressed in either monkey kidney COS7 or murine 3T3 cells (17). By using confocal microscopy, we now show directly that gp91*phox* is expressed on the cell surface in the absence of p22*phox* expression. This result indicates that targeting of gp91*phox* to the plasma membrane does not require heterodimer formation. Recombi-

Table 1. Functional analysis of wild-type and transgenic COS7 cell lines in cell-free NADPH oxidase assays

Source of membranes	O_2^- production*, RLU	O_2^- production†, mmol/min/mg protein
COS7 WT	12,711 ± 27,000 (n = 3)	0.028 ± 0.9 (n = 6)
COS7 gp91	11,111 ± 22,555 (n = 3)	0.13 ± 0.22 (n = 6)
COS7 p22	67,867 ± 7,669 (n = 3)	−0.06 ± 0.03 (n = 6)
COS7 gp91/p22	295,034 ± 81,407 (n = 3)	17.0 ± 0.37 (n = 3)
Neutrophils	538,990 ± 52,888 (n = 3)	88.5 ± 13.3 (n = 3)

*Cell-free assays were performed as described in *Materials and Methods* by using neutrophil or COS7 cell membranes and neutrophil cytosol as a source of cytosolic oxidase components. O_2^- production was monitored by using a chemiluminescence detection system, and the results are expressed as mean ± SEM Tiron-inhibitable relative luminescence units (RLU).

†Cell-free assays were performed as described in *Materials and Methods* by using partially purified neutrophil or COS7 cell membranes and neutrophil cytosol as a source of cytosolic oxidase components. O_2^- production was monitored by using a cytochrome *c* detection system, and the results are expressed as mean ± SEM SOD-inhibitable O_2^- production.

nant gp91^{phox} also was detected in the intracellular membrane compartment in a reticular staining pattern, an appearance consistent with an endoplasmic reticulum–Golgi distribution. Recombinant p22^{phox} expressed in the absence of gp91^{phox} in COS7 cells also was found exclusively in the membrane fraction. However, the diffuse reticular staining pattern seen by using the p22^{phox} mAb, which reacts with an intracellular epitope, made it difficult to determine whether unassembled p22^{phox} was also present in the plasma membrane.

Although a significant amount of research has been focused on understanding the characteristics of the hemes in flavocytochrome b_{558} (11–12, 17–19, 32), the locations of the hemes has remained elusive. As described above, it is now clear that flavocytochrome b_{558} contains two hemes (11). Because the heme groups are not covalently bound in the flavocytochrome molecule and neutrophil flavocytochrome b_{558} loses its heme upon dissociation of the heterodimer (4), it has been difficult to identify directly the heme-binding subunit. Initially, it was suggested that flavocytochrome *b* contained only one heme and that p22^{phox} was the sole heme-containing subunit (18–19). Yamaguchi *et al.* (18) reported the purification of a 20- to 22-kDa heme-containing subunit of flavocytochrome *b*; however, there was a conspicuous absence of gp91^{phox} in their final preparation, and the amino acid composition reported for their protein was significantly different than that determined from the predicted amino acid sequence (33). Nugent *et al.* (19) reported that their experiments using sedimentation equilibrium and radiation inactivation analysis also implicated p22^{phox} as the heme-binding subunit; however, their studies were also subject to methodological problems, including loss of gp91^{phox} from their sample and an inability to reproduce their sedimentation equilibrium results by using gel filtration. In addition, analysis of the p22^{phox} amino acid sequence for heme-coordinating residues demonstrates the presence of only one invariant histidine (20, 33). Thus, it is clear that p22^{phox} could not coordinate a heme by itself. We now know that both gp91^{phox} and p22^{phox} are sensitive to proteolytic degradation, resulting in the formation of $\approx$18−20 kDa fragments without affecting the heme absorbance spectrum (12), so it is possible that the results of these previous studies could have been complicated by the presence of such fragments. Although p22^{phox} was not able to coordinate a heme by itself, it was hypothesized that one of the hemes might be shared between gp91^{phox} and p22^{phox}. In support of this idea, studies by Quinn *et al.* (12) using heme staining of purified neutrophil flavocytochrome separated by lithium dodecyl sulfate/PAGE showed heme staining in bands of 91 and 22 kDa. These results provided evidence for the presence of multiple hemes in flavocytochrome *b*, including a heme bound to gp91^{phox} and a heme possibly shared between both subunits.

In the present studies, the use of transgenic COS7 cell lines has allowed us to obtain direct evidence to further clarify the issue of subunit specificity of the hemes in flavocytochrome b_{558}. Analysis by reduced minus oxidized difference spectroscopy and redox potentiometry clearly showed that gp91^{phox} expressed in COS7 cells in the absence of p22^{phox} probably contains two heme moieties with spectral and redox properties virtually identical to those of neutrophil flavocytochrome b_{558}. The alternative possibility, that gp91^{phox} expressed alone contains only one heme, requires the remarkable coincidence that the midpoint potential of the heme is altered in such a way that it changes from −225 mV or −265 mV to −249 mV. We believe that this is an unlikely scenario and propose that gp91^{phox} is the sole heme-binding subunit of flavocytochrome b_{558}, there being no requirement for a shared heme. A likely explanation for the difference between these studies and the presence of heme-staining in a 22-kDa species is that free heme released during lithium dodecyl sulfate/PAGE may have bound nonspecifically to p22^{phox}. Clearly, there was a significant amount of free heme released during lithium dodecyl sulfate/PAGE, resulting in heme staining at the dye front (12), and it is conceivable that some of this free heme could have bound to smaller proteins in the same gel lane.

The similarities in the spectral data and redox potentiometry in cells expressing gp91^{phox} alone or coexpressing both flavocytochrome b_{558} subunits suggest that formation of a heterodimeric complex with p22^{phox} has little influence on the local environment surrounding the heme groups. We had proposed previously that heme incorporation facilitates heterodimer formation based on our finding that heme availability was essential for the stable expression of p22^{phox} and mature gp91^{phox} in phagocytes (17). The underlying basis for this observation remains uncertain, as is the timing of heme insertion during gp91^{phox} biosynthesis, but is not likely to involve a role for heme as a direct dimerization agent. It is conceivable, however, that heme incorporation into gp91^{phox} produces conformational changes in domains required for heterodimerization with the p22^{phox} subunit.

All of the available optical, EPR, CD, and resonance Raman spectra are consistent with the presence of two, bis-histidinyl, hexacoordinate, low spin hemes within flavocytochrome b_{558} (13, 15, 18, 34, 35). Analysis of hydropathy plots, similarity searches, and our own previous work (11) suggests that the most probable heme axial ligands are His 101 and His 209 (for the heme with Em = −225 mV) and His 115 and His 222 (for the heme with Em = −265 mV) (See Fig. 4). A similar model with a bis-heme motif also has been proposed recently for gp91^{phox}, based on site-directed mutagenesis of histidine residues within the yeast FRE1 iron reductase, a low potential heme protein with sequence and spectral similarities to gp91^{phox} (32, 36). The candidate pairs of histidine residues in gp91^{phox} have the appropriate orientation and spacing to place two heme groups within membrane-spanning α-helices so that electrons could be transferred from FAD to a heme (Em = −225 mV) near the inner face of the membrane and then to the second heme (Em = −265 mV) near the outer face of the membrane, and finally to an extracellular oxygen-binding pocket where O_2^- is formed (37). This type of long range electron transfer or electron tunnelling through the protein has been described previously for other heme proteins (38) and various metalloproteins (39, 40). This model also is supported by the observed effect of an Arg54Ser mutation in gp91^{phox} identified in a patient with X-linked chronic granulomatous disease and a nonfunctional flavocytochrome b_{558} (11). The mutation re-

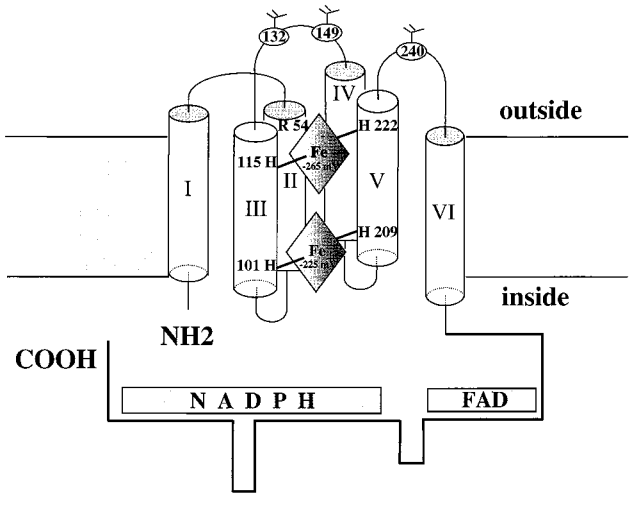

FIG. 4. Model for the location of the two nonidentical hemes in gp91^{phox}. The six transmembranous helices and both NH_2- and COOH-terminal tails are portrayed as indicated. The heme with Em of −265 mV is toward the outer face of the membrane and is coordinated possibly by His 115 and 222. The heme with Em of −225 mV is close to the inner face of the membrane and is coordinated by His 101 and 209. Arg 54 in helix II, which may react with a nearby propionate side chain of the heme (Em = −265 mV), also is shown. The three Asp residues at positions 132, 149, and 240 are indicated as glycosylation sites. Note that the N-terminal Methionine was counted as amino acid #1 in this model, thus explaining the difference between our numbering and that of Wallach *et al.* (38).

duced the Em of the heme with −265 to −300 mV, probably because of an altered interaction between Arg54 with a nearby propionate side chain of the heme (11). Arg54 has been predicted to be at the beginning of the second transmembrane helix, therefore, the heme (Em = −265 mV) is likely close to outer face of the plasma membrane and coordinated by histidines 115 and 222. In this model, the second heme (Em = −225 mV) is coordinated by the other pair of histidine residues (His101 and 209) at the inner face of the cell membrane. Patients with point mutations involving the four potential heme-ligating histidine residues at positions 101, 209, 222 (41), and 115 (A.R.C., D. Noack, J. Rae, and J. Curnutte, unpublished data) of gp91^{phox} are known although in all cases no detectable flavocytochrome b_{558} was expressed and therefore no direct effects on the heme spectrum could be measured. Site directed mutagenesis of these heme-ligating histidine candidates in COS7 cells, followed by spectral analysis and potentiometric titration, may be a potentially powerful alternative approach because mutant derivatives of gp91^{phox} may be more stable in COS7 cells compared with neutrophils.

Coexpression of the flavocytochrome b_{558} subunits gp91^{phox} and p22^{phox} in COS7 cells resulted in the expression of flavocytochrome b_{558} that was functionally capable of supporting O_2^- production in the presence of normal neutrophil cytosol. This finding strongly suggests that the recombinant subunits assemble into a heterodimeric complex in the nonphagocytic COS7 cell background. Neither gp91^{phox} in COS7 gp91 membranes nor p22^{phox} in COS7 p22 membranes was able to replace flavocytochrome b_{558} in a cell-free NADPH oxidase assays, indicating that both flavocytochrome subunits are required for functional assembly of the oxidase. In addition, we have mixed partially purified gp91^{phox} and p22^{phox} from the corresponding COS7 membranes and used in combination with neutrophil cytosol in the cell-free assay but observed no O_2^- formation (not shown). This result indicates that these mixing conditions were not suitable for proper assembly of a functional heterodimer. Another possible explanation is that heterodimer formation is directed by other cellular components *in vivo*, e.g., chaperones, which were not present in our *in vitro* reconstitution experiments. The lower activity of the gp91^{phox}/p22^{phox} heterodimer in COS7 gp91/p22 membranes compared with normal neutrophils could be due to a reduced amount of recombinant flavocytochrome b_{558} present in transgenic COS7 membranes or differences in membrane composition of the different cell types.

In conclusion, the studies presented here strongly suggest that gp91^{phox} is the sole heme binding subunit of the NADPH oxidase that mediates electron transfer in generating O_2^-. However, functional assembly of the active NADPH oxidase requires both subunits of flavocytochrome b_{558}. Domains critical for the normal translocation of cytosolic oxidase components have been identified in both gp91^{phox} and p22^{phox} (2). The associations of p22^{phox} with gp91^{phox}, which are as yet undefined, also may be essential for regulation of electron transfer in the redox cycle or may influence the binding of FAD and/or NADPH. Further studies aimed at identifying the sites of interaction between gp91^{phox} and p22^{phox} may shed light on these issues.

We thank Ruben Sandoval (R.E.B.E.L. Imaging facility, Department of Nephrology) and Laura Nelson (Department of Veterinary Molecular Biology, Montana State University) for expert technical assistance and Kui Shi Voo for helpful discussion in manuscript preparation. This work was supported in part by National Institutes of Health Grants RO1 HL45635 (M.C.D.), RO1 AI24838 (A.R.C.), RO1 AR42426 (M.T.Q.), United States Department of Agriculture Grant NRICGP 9502274 (M.T.Q.), and an Arthritis Foundation Biomedical Science Grant (M.T.Q.). M.T.Q is an Established Investigator of the American Heart Association.

1. Dinauer, M. (1993) *Crit. Rev. Clin. Lab. Sci.* **30,** 329–369.
2. DeLeo, F. & Quinn, M. (1996) *J. Leukocyte Biol.* **60,** 677–691.
3. Cross, A. & Jones, O. T. G. (1991) *Biochem. Biophys. Acta* **1057,** 281–298.
4. Parkos, C., Allen, R., Cochrane, C. & Jesaitis, A. (1987) *J. Clin. Invest.* **80,** 732–742.
5. Huang, J., Hitt, N. & Kleinberg, M. (1995) *Biochemistry* **34,** 16753–16757.
6. Wallach, T. & Segal, A. (1996) *Biochem. J.* **320,** 33–38.
7. Smith, R., Connor, J., Chen, L. & Babior, B. (1996) *J. Clin. Invest.* **98,** 977–983.
8. Segal, A. (1992) *Biochem. J.* **284,** 781–788.
9. Sumimoto, H., Sakamoto, N., Nozaki, M., Sakaki, Y., Takeshige, K. & Minakami, S. (1992) *Biochem. Biophys. Res. Commun.* **186,** 1368–1375.
10. Rotrosen, D., Yeung, C., Leto, T., Malech, H. & Kwong, C. (1992) *Science* **256,** 1459–1462.
11. Cross, A., Rae, J. & Curnutte, J. (1995) *J. Biol. Chem.* **270,** 17075–17077.
12. Quinn, M., Mullen, M. & Jesaitis, A. (1992) *J. Biol. Chem.* **267,** 7303–7309.
13. Hurst, J., Loehr, T., Curnutte, J. & Rosen, H. (1991) *J. Biol. Chem.* **266,** 1627–1634.
14. Ueno, I., Fujii, S., Ohya-Nishiguchi, H., Iizuka, T. & Kanegasaki, S. (1991) *FEBS Lett.* **281,** 130–132.
15. Miki, T., Fujii, H. & Kakinuma, K. (1992) *J. Biol. Chem.* **267,** 19673–19675.
16. Parkos, C., Dinauer, M., Jesaitis, A., Orkin, S. & Curnutte, J. (1989) *Blood* **73,** 1416–1420.
17. Yu, L., Zhen, L. & Dinauer, M. (1997) *J. Biol. Chem.* **272,** 27288–27294.
18. Yamaguchi, T., Hayakawa, T., Kaneda, M., Kakinuma, K. & Yoshikawa, A. (1989) *J. Biol. Chem.* **264,** 112–118.
19. Nugent, J., Gratzer, W. & Segal, A. (1989) *Biochem. J.* **264,** 921–924.
20. Dinauer, M., Pierce, E., Bruns, G., Curnutte, J. & Orkin, S. (1990) *J. Clin. Invest.* **86,** 1729–1737.
21. Yu, L., Takeshige, K., Nunoi, H. & Minakami, S. (1993) *Biochem. Biophys. Acta* **1178,** 73–80.
22. Nakamura, M., Murakami, M., Koga, T., Tanaka, Y. & Minakami, S. (1987) *Blood* **69,** 1404–1408.
23. Nakamura, M., Sendo, S., van Zwieten, R., Koga, T., Roos, D. & Kanegasaki, S. (1988) *Blood* **72,** 1550–1552.
24. Verhoeven, A., Bolscher, B., Meerhof, L., van Zwieten, R., Keijer, J., Weening, R. & Roos, D. (1989) *Blood* **73,** 1686–1694.
25. Ginsel, L., Onderwater, J., Fransen, J., Verhoeven, A. & Roos, D. (1990) *Blood* **76,** 2105–2116.
26. Zhen, L., Yu, L. & Dinauer, M. (1998) *J. Biol. Chem.* **273,** 6575–6581.
27. Cross, A., Higson, F., Jones, O. T. G., Harper, A. & Segal, A. (1982) *Biochem. J.* **204,** 479–485.
28. Cross, A., Jones, O. T. G., Harper, A. & Segal, A. (1981) *Biochem. J.* **194,** 599–606.
29. Cross, A. & Curnutte, J. (1995) *J. Biol. Chem.* **270,** 6543–6548.
30. Nishinaka, Y., Aramaki, Y., Yoshida, H., Masuya, H., Sugawara, T. & Ichimori, Y. (1998) *Biochem. Biophys. Res. Commun.* **193,** 554–559.
31. Porter, C., Parkar, M., Verhoeven, A., Levinsky, R., Collins, M. & Kinnon, C. (1994) *Blood* **84,** 2767–2775.
32. Finegold, A., Shatwell, K., Segal, A., Klausner, R. & Dancis, A. (1996) *J. Biol. Chem.* **271,** 31021–31024.
33. Parkos, C., Dinauer, M., Walker, L., Allen, R., Jesaitis, A. & Orkin, S. (1988) *Proc. Natl. Acad. Sci. USA* **85,** 3319–3323.
34. Iizuka, T., Kanegasaki, S., Makino, R., Tanaka, T. & Ishimura, Y. (1985) *J. Biol. Chem.* **260,** 12049–12053.
35. Isogai, Y., Iizuka, T., Makino, R., Iyanagi, T. & Orii, Y. (1993) *J. Biol. Chem.* **268,** 4025–4031.
36. Shatwell, K., Dancis, A., Cross, A., Klausner, R. & Segal, A. (1996) *J. Biol. Chem.* **271,** 14240–14244.
37. Fujii, H. & Kakinuma, K. (1990) *J. Biochem.* **108,** 292–296.
38. Mayo, S., Ellis, W., Crutchley, R. & Gray, H. (1986) *Science* **233,** 948–952.
39. Gray, H. & Winkler, J. (1996) *Annu. Rev. Biochem.* **65,** 537–561.
40. Cowan, J., Upmacis, R., Beratan, D., Onuchic, J. & Gray, H. (1988) *Ann. N. Y. Acad. Sci.* **550,** 68–84.
41. Roos, D., de Boer, M., Kuribayashi, F., Meischl, C., Weening, R., Segal, A., Ahlin, A., Nemet, K., Hossle, J., Bernatowska-Matuszkiewicz, E., *et al.* (1996) *Blood* **87,** 1663–1681.
42. Wallach, T. & Segal, A. (1997) *Biochem. J.* **321,** 583–585.